HHS Public Access

Author manuscript

Cell Rep. Author manuscript; available in PMC 2017 October 17.

Published in final edited form as:

Cell Rep. 2016 June 14; 15(11): 2315–2322. doi:10.1016/j.celrep.2016.05.075.

Western Zika Virus in Human Fetal Neural Progenitors Persists Long Term with Partial Cytopathic and Limited Immunogenic Effects

Natasha W. Hanners[1,2], **Jennifer L. Eitson**[1], **Noriyoshi Usui**[3], **R. Blake Richardson**[1], **Eric M. Wexler**[4], **Genevieve Konopka**[3], and **John W. Schoggins**[1,*]

[1]Department of Microbiology, University of Texas Southwestern Medical Center, Dallas, TX 75390, USA

[2]Division of Infectious Disease, Department of Pediatrics, University of Texas Southwestern Medical Center, Dallas, TX 75390, USA

[3]Department of Neuroscience, University of Texas Southwestern Medical Center, Dallas, TX 75390, USA

[4]Department of Psychiatry, David Geffen School of Medicine, University of California, Los Angeles, Los Angeles, CA 90095, USA

SUMMARY

The recent Zika virus (ZIKV) outbreak in the Western hemisphere is associated with severe pathology in newborns, including microcephaly and brain damage. The mechanisms underlying these outcomes are under intense investigation. Here, we show that a 2015 ZIKV isolate replicates in multiple cell types, including primary human fetal neural progenitors (hNPs). In immortalized cells, ZIKV is cytopathic and grossly rearranges endoplasmic reticulum membranes similar to other flaviviruses. In hNPs, ZIKV infection has a partial cytopathic phase characterized by cell rounding, pyknosis, and activation of caspase 3. Despite notable cell death, ZIKV did not activate a cytokine response in hNPs. This lack of cell intrinsic immunity to ZIKV is consistent with our observation that virus replication persists in hNPs for at least 28 days. These findings, supported by published fetal neuropathology, establish a proof-of-concept that neural progenitors in the developing human fetus can be direct targets of detrimental ZIKV-induced pathology.

In Brief

*Correspondence: john.schoggins@utsouthwestern.edu.

SUPPLEMENTAL INFORMATION

Supplemental Information contains Supplemental Experimental Procedures and two figures and can be found with this article online at http://dx.doi.org/10.1016/j.celrep.2016.05.075.

AUTHOR CONTRIBUTIONS

N.W.H., G.K., and J.W.S. designed the study. N.W.H., J.L.E., N.U., R.B.R., and J.W.S. performed the experiments. E.M.W. and G.K. provided critical reagents. All authors analyzed the data. N.W.H. and J.W.S. drafted the manuscript, and all authors edited the paper.

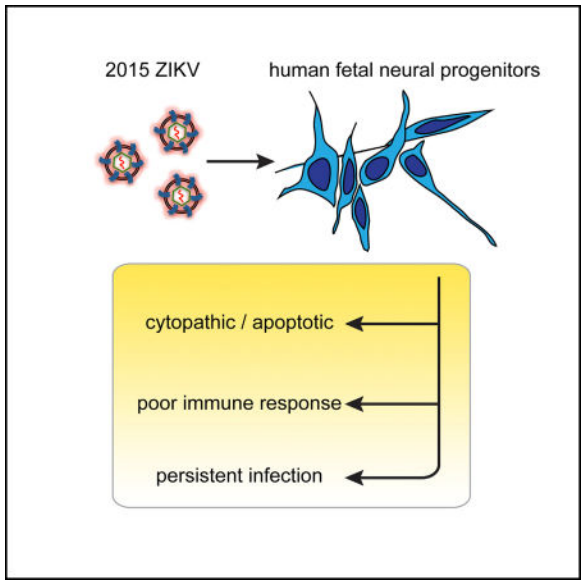

Hanners et al. establish a cell-culture model of a 2015 ZIKV isolate in primary human fetal neural progenitors. They show that ZIKV infection kills a subset of fetal neural progenitors with limited activation of inflammatory or immune responses. In the surviving neural progenitors, ZIKV replication persists for many weeks, mirroring fetal neuropathological findings in vivo.

INTRODUCTION

Zika virus (ZIKV) is a positive-sense, single-stranded RNA virus in the *Flaviviridae* family. In 2015, the detection of circulating ZIKV in Brazil later coincided with an alarming increase in the number of babies born with microcephaly (Kindhauser et al., 2016; Schuler-Faccini et al., 2016). Accumulating evidence has now been deemed sufficiently strong to establish a causal relationship between maternal ZIKV infection and microcephaly and other fetal brain anomalies (Rasmussen et al., 2016). In adults, 93% of patients diagnosed with Guillain-Barré syndrome during the French Polynesia outbreak of 2013 were positive for ZIKV IgM (Cao-Lormeau et al., 2016). These findings indicate that contemporary ZIKV is highly neurovirulent, with particularly devastating consequences in fetuses.

Cell cultures and animal models have begun to reveal mechanisms of ZIKV-induced pathology. Recent studies have reported that ZIKV infects stem-cell-derived human neural progenitors (hNPs), neurospheres, and organoids with growth-attenuating effects (Cugola et al., 2016; Dang et al., 2016; Garcez et al., 2016; Qian et al., 2016; Tang et al., 2016). African and Asian ZIKV infections do not infect full-term primary human placental trophoblasts due to type III interferon-mediated viral restriction (Bayer et al., 2016). In mouse models, some of which are immunocompromised, ZIKV infections recapitulate multiple features of disease in humans, including trans-placental fetal transmission and severe neuropathology in both the adult and fetal brain (Cugola et al., 2016; Lazear et al., 2016; Li et al., 2016; Miner et al., 2016; Rossi et al., 2016; Wu et al., 2016). Comparative viral sequence analyses revealed that multiple amino-acid changes have arisen over the past half century as the virus has migrated out of Africa (Wang et al., 2016). Several mutations are predicted to cause

significant changes in protein structure, underscoring the importance of studying ZIKV isolates from the current outbreak.

Here, we use immortalized cell cultures and fetal-derived hNPs to characterize a contemporary ZIKV isolate from the current outbreak in the Western hemisphere. We show that ZIKV is acutely cytopathic in neural progenitors but establishes a persistent infection that is consistent with clinical pathology findings (Driggers et al., 2016; Mlakar et al., 2016; Rasmussen et al., 2016). We also demonstrate that neural progenitors are poorly immunogenic in response to ZIKV.

RESULTS

Characterization of a 2015 ZIKV Isolate

We obtained a ZIKV strain isolated from Puerto Rico in 2015 (ZIKV-PRVABC59) and propagated multiple stocks on Vero-E6 cells. Given that the virus formed small, poorly demarcated plaques in these cells (data not shown), we plaqued the viral stock on baby hamster kidney (BHK-21J) cells. Small, discernable plaques were visualized 4 days after infection (Figure 1A), and viral titers from three independent preps were approximately 1.0×10^7 plaque forming units (pfu) per ml. In comparison to ZIKV, the related flavivirus yellow fever virus (YFV) formed large plaques under identical assay conditions (Figure 1A). Next, we assessed ZIKV infectivity in multiple cell lines using an antibody (4G2) that detects the dengue virus (DENV) envelope and cross-reacts with ZIKV (Hamel et al., 2015). At 24 hr after infection, we observed positive antigen staining by immunofluorescence in diverse cell types, including Vero-E6 cells, BHK-21J, Huh7.5, and *STAT1*$^{-/-}$ human fibroblasts (data not shown) (Figure 1B). We also assessed ZIKV infection by flow cytometry. Viral antigen was detected in Huh7.5 cells at 24 hr after infection, and considerable viral spread occurred by 48 hr (Figure 1C). Using a fluorescence-activated cell sorting (FACS)-based viral titering assay, a ZIKV growth curve in Huh7.5 cells revealed that that the complete viral lifecycle of this isolate is just under 20 hr. (Figure 1D). Given that the 4G2 cross-reacts to both ZIKV from DENV, we also established a qRT-PCR assay to distinguish these two viruses (Figure S1A).

Ultrastructural Analysis of Viral Replication

Electron microscopy has been used to detect viral particles in brain tissue from fetuses with ZIKV infection (Driggers et al., 2016; Mlakar et al., 2016). Although these studies did not use immunolabeling to confirm ZIKV, they did show viral particles and lipid rearrangements characteristic of flavivirus infection. We used electron microscopy in Huh7.5 cells to compare at the ultrastructural level three flavivirus infections: DENV (serotype 2, strain 16681), YFV (strain 17D), and ZIKV. Consistent with previous reports (Junjhon et al., 2014; Welsch et al., 2009), DENV infection resulted in endoplasmic reticulum membrane rearrangements characterized by packets of single-membrane vesicles or so-called “replication complexes” and larger, gross perturbations referred to as “convoluted membranes” (Figure 1E). Similar to DENV, YFV infection induced vesicle formation at the ER. However, we rarely observed convoluted membranes in YFV-infected cells. ZIKV-infected cells had both vesicle packets and convoluted membranes (Figures 1E and S1B),

suggesting that ZIKV causes cytoplasmic membrane rearrangements that are more similar to DENV than YFV. We also noted that ZIKV and DENV induce the formation of large (>200 nm) invaginated vacuoles that resemble expanded versions of the smaller replication complexes (Figure S1B). Across all experiments, we frequently detected YFV particles and occasionally observed DENV particles but were unable to find ZIKV particles (Figure S1B). These findings are consistent with our observation that YFV replicates more robustly than ZIKV (Figure 1A).

ZIKV Replicates in Primary hNPs

Recent studies have shown that the prototype and contemporary ZIKV strains can infect neural progenitors, neurospheres, and organoids derived from human induced pluripotent stem cells (iPSCs) or embryonic stem cells (Cugola et al., 2016; Dang et al., 2016; Garcez et al., 2016; Qian et al., 2016; Tang et al., 2016). However, stem-cell-derived neural progenitors do not consistently recapitulate in vivo embryonic human brain gene expression as well as fetal brain-derived primary hNPs (Stein et al., 2014). Moreover, hNPs are directly obtained from the tissue of interest with respect to ZIKV pathophysiology, the human fetal brain, whereas iPSCs are derived from non-neural tissue and might not model all aspects of in vivo neural cell function with regards to ZIKV tropism. Thus, we sought to determine whether hNPs were susceptible to the 2015 Puerto Rican ZIKV isolate. We obtained two fetal hNP lines that were acquired at 16–19 weeks of gestation, a time-frame of fetal development that correlates with risk for severe fetal neurologic complications after ZIKV exposure (Rasmussen et al., 2016). hNP cultures were infected with ZIKV at 0.5 MOI and processed for immunofluorescence 72 hr after infection in order to detect viral antigen and the neuronal marker nestin. In both lines, all cells expressed nestin, and numerous cells stained positive for ZIKV infection (Figure 2A). When infection levels were quantified by FACS, we found that approximately 15% of hNPs were ZIKV-positive 48 hr after infection (Figures 2B and 2C).

ZIKV Is Partly Cytopathic, but Poorly Immunogenic, in hNP

Microscopic analysis of ZIKV-infected hNPs revealed that cytopathic effects were evident as early as day 2 and more pronounced at later time points (Figure 3). These cytopathic effects appeared similar to those observed in Huh7.5 and *STAT1*$^{-/-}$ fibroblasts (Figure 3A) (data not shown). Cell death in hNPs correlated with an increase in the presence of pyknotic nuclei (Figure 3B), which were only rarely visualized in uninfected hNPs (data not shown). Using immunofluorescence, we found that hNPs with pkynotic nuclei were typically also positive for ZIKV antigen and activated caspase 3 (Figure 3C). These data indicate that the mechanism of ZIKV-induced cell death is mot likely though an apoptotic pathway.

To determine whether the apoptotic phenotype correlated with an inflammatory response, we used an antibody-based array to simultaneously detect more than 102 human cytokines and chemokines. Although multiple cytokines and growth factors were secreted by hNPs (or present in the culture media), we found no difference between mock-infected and ZIKV-infected cultures (Figure S2A). To confirm the array, we used the more sensitive ELISA to quantify secreted TNFα, a proinflammatory cytokine, CCL2, a proinflammatory chemokine, and CX3CL1, a neuroprotective chemokine that is released from neurons after toxic insults

(Conductier et al., 2010; Limatola and Ransohoff, 2014). In addition to ZIKV infection, we also treated cells with the viral double-stranded RNA mimic polyinosinic-polycytidylic acid (pIC) and the endotoxin lipopolysaccharide (LPS). At 24 hr after treatment, pIC robustly induced TNFα and CCL2 and moderately induced CXCL3, indicating that the cells are responsive to immunostimulatory ligands (Figure 3D). By contrast, LPS and ZIKV did not stimulate cytokine secretion in hNPs. We confirmed the lack of ZIKV stimulation by ELISA in a second hNP line at both 24 and 72 hr after infection (Figures S2B and S2C). We also confirmed LPS bioactivity by monitoring TNFα and CCL2 induction in THP-1 human monocytic cells (Figure 3D). Similar to hNPs, ZIKV did not stimulate cytokine secretion in THP-1 cells. Although type I IFNs were not on the cytokine array, we tested hNP and THP-1 supernatants for IFNα secretion using ELISA. In all conditions, the IFNα signal was below the assay's limit of detection (data not shown).

We corroborated the ELISA data by measuring cytokine mRNA induction in hNPs and THP-1 cells. Overall, the data from qRT-PCR assays were similar to the ELISA results. pIC induced *TNFA, CCL2*, and *IFNB*, but not *IFNA*, (Figure 3E). LPS and ZIKV did not induce cytokine mRNA in hNPs, although LPS readily induced cytokine mRNA in THP-1 cells. In both cell types, we confirmed ZIKV infection using ZIKV-specific primers. Together, these results indicate that, although hNPs are immunoresponsive to a viral RNA mimic (pIC), under these experimental conditions, they are refractory to the induction of neuroinflammatory or neuroprotective cytokines in response to ZIKV.

Persistent ZIKV Production in hNPs

To determine whether the hypoimmune status of hNPs in response to ZIKV impacted virus replication long term, we monitored virus production in hNPs over a 28 or 12 day timecourse for hNP lines 1 and 2, respectively. Cells were infected with 0.5 MOI ZIKV, and viral titers in hNP supernatants were determined on naive Huh7.5 cell using FACS-based titering (Figure 4). In hNP line 1, we detected an early rise in viral titers that peaked 3 days after infection. This phase of virus production was followed by a drop in titer that coincides with the peak of the cytopathic effect. Viral titers peaked again at day 7 and remained at this level until day 20, when titers rose slightly for the remainder of the 28 day timecourse. In hNP line 2, a similar trend was observed. These data indicate that, after an initial cytotoxic phase, ZIKV establishes a persistent infection in this hNP culture model.

DISCUSSION

Here, we characterized a contemporary 2015 isolate of ZIKV in cell culture. Similar to other strains of ZIKV, PRVABC59 infects multiple immortalized cell types and causes classical cytopathic effects. At the ultrastructural level, ZIKV appears to alter cellular membranes similar to DENV. To develop a cell-culture model of ZIKV-host interactions that most closely mimics native ZIKV tropism in utero, we used primary fetal hNPs. We found that ZIKV infects hNPs at a relatively low frequency (on average less than 20% of cells). The initial acute phase of infection was characterized by cytopathic effects in a subset of cells, with cell rounding, pkynotic nuclei, and positive staining for activated caspase 3. Occasionally, activated caspase 3 was observed in ZIKV-negative cells that were in close

proximity to an infected cell, suggesting that apoptotic pathways in hNPs may be activated through both cell-intrinsic and -extrinsic mechanisms. However, regarding the latter, we were unable to detect the production of proinflammatory cytokines, chemokines, or antiviral IFNs in ZIKV-infected hNP supernatants at 24 hr or 72 hr after infection. Although a short-lived response at earlier time points may have been missed under our experimental conditions, the lack of virus-induced cytokine protein accumulation at 24 hr suggests that hNPs have limited immunogenic effects in response to ZIKV. However, hNPs can mount immune responses since they responded robustly to a viral RNA mimic. Thus, our data indicate that, although ZIKV causes cell death in hNPs, either the virus is relatively stealthy with respect to modulating immune pathways or isolated hNPs possess an inherent hypoimmunogenicity with respect to ZIKV infection. This latter speculation is supported by previous studies characterizing neural progenitors as possessing inherent immune privilege in experimental allograft models (Hori et al., 2003). Additional studies in hNPs are needed to test these hypotheses. Moreover, given that our hNP cell-culture model is a reductionist system, comprehensive immunopathological studies in ZIKV-infected fetal brain tissue are also needed. It is likely that glial progenitors and microglia, the main producers of inflammatory mediators in the brain, will also play a role in the pathophysiology of ZIKV in vivo.

We also found that ZIKV persistently replicates in hNPs. After the initial cytopathic phase, a proportion of cells survive and continue to produce the virus. We confirmed this in two independent hNP lines, with one line producing virus for up to 28 days. This observation correlates with clinical pathological findings in infected fetuses (Driggers et al., 2016; Mlakar et al., 2016). In one study, ZIKV particles were observed in fetal brain tissue 19 weeks after presumed maternal infection (Mlakar et al., 2016). Thus, our hNP model of ZIKV infection mirrors viral persistence in vivo. The exact nature of this persistence remains to be determined. Specifically, we do not know whether the persistently produced virus results from a focal infection (i.e., only a few cells) or a diffuse, steady-state infection or whether replicated virus segregates to daughter cells during cell division.

Beyond neuronal cells, recent studies on ZIKV sexual transmission suggest viral persistence outside the CNS, namely the testes. Indeed, infectious ZIKV has been isolated from the semen of an infected male several weeks after the onset of symptoms (Mansuy et al., 2016). In support of these findings, in ZIKV-infected mice high viral titers were found 6 days after infection in not only in the brain and spinal cord but also the testes (Lazear et al., 2016). Other studies have reported ZIKV-induced disorders of the retina (de Paula Freitas et al., 2016; Ventura et al., 2016), suggesting either direct or indirect effects of ZIKV in certain ocular cell types. Thus, the process that seems to unify ZIKV tropism, persistence, and both vertical and sexual transmission is access to sites of immune privilege (fetus, eyes, and testes). Similar to our hNP model, these sites may be immunotolerant to ZIKV, thereby increasing the potential for viral persistence and pathological sequelae.

Although ZIKV infection in hNPs models certain aspects of clinical pathological findings (neuronal death followed by persistent virus replication), many questions remain unanswered. It is tempting to speculate that the mechanisms underlying ZIKV-induced microcephaly are simply due to direct injury to neural progenitor cells, as used in our study,

or to progenitor cells in the brain such as radial glial cells (Nowakowski et al., 2016). However, the pathology may be more complex and include direct or indirect effects on neuronal progenitor proliferation or symmetric or asymmetric division, neuronal differentiation or migration, and/or neuron-glial interactions (Cugola et al., 2016; Li et al., 2016). The hNP culture system has been previously validated for its utility in generating neurons at various stages of differentiation (Konopka et al., 2012; Stein et al., 2014). Thus, future studies that take advantage of these features of the hNP culture system may be instrumental in uncovering molecular mechanisms underlying the pathophysiological effects of ZIKV.

EXPERIMENTAL PROCEDURES

Cells and Viruses

Cell cultures and viral stocks were generated with standard techniques. See the Supplemental Information for details.

Virus Infections and Titer Determination

For FACS and viral growth-curve experiments, cells were plated in 24-well plates at 100,000–150,000 cells per well. Cells were infected with ZIKV at an MOI of 0.5 for 1 hr at 37°C under 5% CO_2. At indicated times, cells were harvested using Accumax (Sigma-Aldrich) and fixed using a BD Cytofix/Cytoperm kit (Fisher Scientific). Cells were stained with primary antibody, anti-flavivirus group antigen antibody, clone D1-4G2-4-15 (Millipore), and secondary antibody, goat anti-mouse IgG (H+L) Alexa Fluor 488 (Life Technologies). Samples were run on an S1000 flow cytometer (Stratedigm) and analyzed in FlowJo. For Huh7.5 and hNP viral growth curves, cells were infected with 0.5 MOI ZIKV, washed three times with PBS+/+, and incubated in DMEM (Huh7.5) or hNP-proliferation media for the indicated time. Supernatants were collected and stored at −80°C. Thawed supernatants were centrifuged in order to remove cell debris and titered on Huh7.5 cells. See the Supplemental Information for details on viral titering assays.

Indirect Immunofluorescence

Immortalized cells and hNP lines were infected with ZIKV and processed for antibody staining by immunofluorescence. See the Supplemental Information for details.

Electron Microscopy

Huh7.5 cells were infected with 1.5 MOI YFV for 24 hr, 3 MOI DENV for 48 hr, 4 MOI ZIKV for 24 hr, or 1 MOI ZIKV for 48 hr and processed for transmission electron microscopy. See the Supplemental Information for details.

Cytokine Arrays and ELISA

Cell supernatants were collected 24 or 72 hr after infection and frozen at −80°C. Thawed samples were applied to Human XL Cytokine Array (ARY022, R&D Systems) per kit protocols. For increased sensitivity, the maximum volume of supernatant (500 μl) was used

on the array. ELISA kits to detect TNFα, CCL2, and CXCL3 (R&D Systems) or IFNα (PBL Assay Science) were used according to the manufacturer's protocol.

RT-PCR of Viral Genomes and Cellular Genes

Huh7.5 cells were infected with titrating doses of DENV-IC30-P-A or ZIKV for 1 hr. hNP were infected with 0.5 MOI ZIKV, treated with 10 ng/ml pIC (Invivogen), or treated with 100 ng/ml LPS (Sigma-Aldrich). Total RNA was extracted 24 hr later using an RNeasy Mini Kit (QIAGEN). 50 ng total RNA was used in QuantiTect SYBR Green RT-PCR reactions (QIAGEN) in order to detect the following viral or cellular mRNAs: ZIKV, DENV, *TNFA, CCL2, IFNA, IFNB*, and *RPS11*. All samples were normalized to housekeeping gene *RPS11*. Samples were run on 7500 Fast Real-Time PCR System (Life Technologies). Primer information is available upon request.

Statistical Analysis

For FACS-based analysis of hNP infectivity, statistical analysis was determined by Mann-Whitney test. For ELISA assays to measure cytokines in hNPs, statistical significance was determined by one-way ANOVA with Dunnett's test for multiple comparisons. For RT-PCR assays to measure cytokine mRNA or ZIKV RNA, statistical significance was determined by one-way ANOVA with Kruskal-Wallis' test (non-parametric) for multiple comparisons.

Supplementary Material

Refer to Web version on PubMed Central for supplementary material.

Acknowledgments

We thank Katrina Mar for technical advice and the UT Southwestern Electron Microscopy Core Facility for technical support. This work was supported in part by NIH grants DK095031 (J.W.S.), AI117922 (J.W.S.), MH102603 (G.K.), and a grant from the Rita Allen Foundation (J.W.S.). The content is solely the responsibility of the authors and does not necessarily represent the official views of the NIH or the other funders.

References

Bayer A, Lennemann NJ, Ouyang Y, Bramley JC, Morosky S, Marques ET Jr, Cherry S, Sadovsky Y, Coyne CB. Type III Interferons Produced by Human Placental Trophoblasts Confer Protection against Zika Virus Infection. Cell Host Microbe. 2016; 19:705–712. [PubMed: 27066743]

Cao-Lormeau VM, Blake A, Mons S, Lastère S, Roche C, Vanhomwegen J, Dub T, Baudouin L, Teissier A, Larre P, et al. Guillain-Barré Syndrome outbreak associated with Zika virus infection in French Polynesia: a case-control study. Lancet. 2016; 387:1531–1539. [PubMed: 26948433]

Conductier G, Blondeau N, Guyon A, Nahon JL, Rovère C. The role of monocyte chemoattractant protein MCP1/CCL2 in neuroinflammatory diseases. J. Neuroimmunol. 2010; 224:93–100. [PubMed: 20681057]

Cugola, FR., Fernandes, IR., Russo, FB., Freitas, BC., Dias, JLM., Guimarães, KP., Benazzato, C., Almeida, N., Pignatari, GC., Romero, S., et al. The Brazilian Zika virus strain causes birth defects in experimental models. Nature. 2016. Published online May 11, 2016. http://dx.doi.org/10.1038/nature18296

Dang, J., Tiwari, SK., Lichinchi, G., Qin, Y., Patil, VS., Eroshkin, AM., Rana, TM. Zika Virus Depletes Neural Progenitors in Human Cerebral Organoids through Activation of the Innate Immune Receptor TLR3. Cell Stem Cell. 2016. Published online May 6, 2016. http://dx.doi.org/10.1016/j.stem.2016.04.014

de Paula Freitas, B., de Oliveira Dias, JR., Prazeres, J., Sacramento, GA., Ko, AI., Maia, M., Belfort, R, Jr. Ocular findings in infants with microcephaly associated with presumed Zika virus congenital infection in Salvador, Brazil. JAMA Ophthalmol. 2016. http://dx.doi.org/10.1001/jamaophthalmol.2016.0267

Driggers, RW., Ho, CY., Korhonen, EM., Kuivanen, S., Jääskeläinen, AJ., Smura, T., Rosenberg, A., Hill, DA., DeBiasi, RL., Vezina, G., et al. Zika virus infection with prolonged maternal viremia and fetal brain abnormalities. N. Engl. J. Med. 2016. Published online March 30, 2016. http://dx.doi.org/10.1056/NEJMoa1601824

Garcez PP, Loiola EC, Madeiro da Costa R, Higa LM, Trindade P, Delvecchio R, Nascimento JM, Brindeiro R, Tanuri A, Rehen SK. Zika virus impairs growth in human neurospheres and brain organoids. Science. 2016; 352:816–818. [PubMed: 27064148]

Hamel R, Dejarnac O, Wichit S, Ekchariyawat P, Neyret A, Luplertlop N, Perera-Lecoin M, Surasombatpattana P, Talignani L, Thomas F, et al. Biology of Zika Virus Infection in Human Skin Cells. J. Virol. 2015; 89:8880–8896. [PubMed: 26085147]

Hori J, Ng TF, Shatos M, Klassen H, Streilein JW, Young MJ. Neural progenitor cells lack immunogenicity and resist destruction as allografts. Stem Cells. 2003; 21:405–416. [PubMed: 12832694]

Junjhon J, Pennington JG, Edwards TJ, Perera R, Lanman J, Kuhn RJ. Ultrastructural characterization and three-dimensional architecture of replication sites in dengue virus-infected mosquito cells. J. Virol. 2014; 88:4687–4697. [PubMed: 24522909]

Kindhauser, MK., Allen, T., Frank, V., Santhana, RS., Dye, C. Bulletin of the World Health Organization; 2016. Zika: The origin and spread of a mosquito-borne virus.

Konopka G, Wexler E, Rosen E, Mukamel Z, Osborn GE, Chen L, Lu D, Gao F, Gao K, Lowe JK, Geschwind DH. Modeling the functional genomics of autism using human neurons. Mol. Psychiatry. 2012; 17:202–214. [PubMed: 21647150]

Lazear HM, Govero J, Smith AM, Platt DJ, Fernandez E, Miner JJ, Diamond MS. A Mouse Model of Zika Virus Pathogenesis. Cell Host Microbe. 2016; 19:720–730. [PubMed: 27066744]

Li, C., Xu, D., Ye, Q., Hong, S., Jiang, Y., Liu, X., Zhang, N., Shi, L., Qin, CF., Xu, Z. Zika Virus Disrupts Neural Progenitor Development and Leads to Microcephaly in Mice. Cell Stem Cell. 2016. Published online May 9, 2016. http://dx.doi.org/10.1016/j.stem.2016.04.017

Limatola C, Ransohoff RM. Modulating neurotoxicity through CX3CL1/CX3CR1 signaling. Front. Cell. Neurosci. 2014; 8:229. [PubMed: 25152714]

Mansuy JM, Dutertre M, Mengelle C, Fourcade C, Marchou B, Delobel P, Izopet J, Martin-Blondel G. Zika virus: high infectious viral load in semen, a new sexually transmitted pathogen? Lancet Infect. Dis. 2016; 16:405.

Miner JJ, Cao B, Govero J, Smith AM, Fernandez E, Cabrera OH, Garber C, Noll M, Klein RS, Noguchi KK, et al. Zika Virus Infection during Pregnancy in Mice Causes Placental Damage and Fetal Demise. Cell. 2016; 165:1081–1091. [PubMed: 27180225]

Mlakar J, Korva M, Tul N, Popović M, Poljšak-Prijatelj M, Mraz J, Kolenc M, Resman Rus K, Vesnaver Vipotnik T, Fabjan Vodušek V, et al. Zika Virus Associated with Microcephaly. N. Engl. J. Med. 2016; 374:951–958. [PubMed: 26862926]

Nowakowski TJ, Pollen AA, Di Lullo E, Sandoval-Espinosa C, Bershteyn M, Kriegstein AR. Expression Analysis Highlights AXL as a Candidate Zika Virus Entry Receptor in Neural Stem Cells. Cell Stem Cell. 2016; 18:591–596. [PubMed: 27038591]

Qian X, Nguyen HN, Song MM, Hadiono C, Ogden SC, Hammack C, Yao B, Hamersky GR, Jacob F, Zhong C, et al. Brain-Region-Specific Organoids Using Mini-bioreactors for Modeling ZIKV Exposure. Cell. 2016; 165:1238–1254. [PubMed: 27118425]

Rasmussen SA, Jamieson DJ, Honein MA, Petersen LR. Zika Virus and Birth Defects–Reviewing the Evidence for Causality. N. Engl. J. Med. 2016; 374:1981–1987. [PubMed: 27074377]

Rossi SL, Tesh RB, Azar SR, Muruato AE, Hanley KA, Auguste AJ, Langsjoen RM, Paessler S, Vasilakis N, Weaver SC. Characterization of a Novel Murine Model to Study Zika Virus. Am. J. Trop. Med. Hyg. 2016:16–0111. [PubMed: 28077739]

Schuler-Faccini L, Ribeiro EM, Feitosa IM, Horovitz DD, Cavalcanti DP, Pessoa A, Doriqui MJ, Neri JI, Neto JM, Wanderley HY, et al. Brazilian Medical Genetics Society–Zika Embryopathy Task

Force. Possible Association Between Zika Virus Infection and Microcephaly - Brazil, 2015. MMWR Morb. Mortal. Wkly. Rep. 2016; 65:59–62. [PubMed: 26820244]

Stein JL, de la Torre-Ubieta L, Tian Y, Parikshak NN, Hernández IA, Marchetto MC, Baker DK, Lu D, Hinman CR, Lowe JK, et al. A quantitative framework to evaluate modeling of cortical development by neural stem cells. Neuron. 2014; 83:69–86. [PubMed: 24991955]

Tang H, Hammack C, Ogden SC, Wen Z, Qian X, Li Y, Yao B, Shin J, Zhang F, Lee EM, et al. Zika Virus Infects Human Cortical Neural Progenitors and Attenuates Their Growth. Cell Stem Cell. 2016; 18:587–590. [PubMed: 26952870]

Ventura CV, Maia M, Bravo-Filho V, Góis AL, Belfort R Jr. Zika virus in Brazil and macular atrophy in a child with microcephaly. Lancet. 2016; 387:228.

Wang L, Valderramos SG, Wu A, Ouyang S, Li C, Brasil P, Bonaldo M, Coates T, Nielsen-Saines K, Jiang T, et al. From Mosquitos to Humans: Genetic Evolution of Zika Virus. Cell Host Microbe. 2016; 19:561–565. [PubMed: 27091703]

Welsch S, Miller S, Romero-Brey I, Merz A, Bleck CK, Walther P, Fuller SD, Antony C, Krijnse-Locker J, Bartenschlager R. Composition and three-dimensional architecture of the dengue virus replication and assembly sites. Cell Host Microbe. 2009; 5:365–375. [PubMed: 19380115]

Wu, KY., Zuo, GL., Li, XF., Ye, Q., Deng, YQ., Huang, XY., Cao, WC., Qin, CF., Luo, ZG. Vertical transmission of Zika virus targeting the radial glial cells affects cortex development of offspring mice. Cell Res. 2016. http://dx.doi.org/10.1038/cr.2016.58

Author Manuscript

Author Manuscript

Author Manuscript

Highlights

- A 2015 ZIKV isolate replicates in human fetal neural progenitors
- ZIKV in fetal neural progenitors is partially cytopathic and persists for weeks
- ZIKV has limited immunogenic effects in fetal neural progenitors

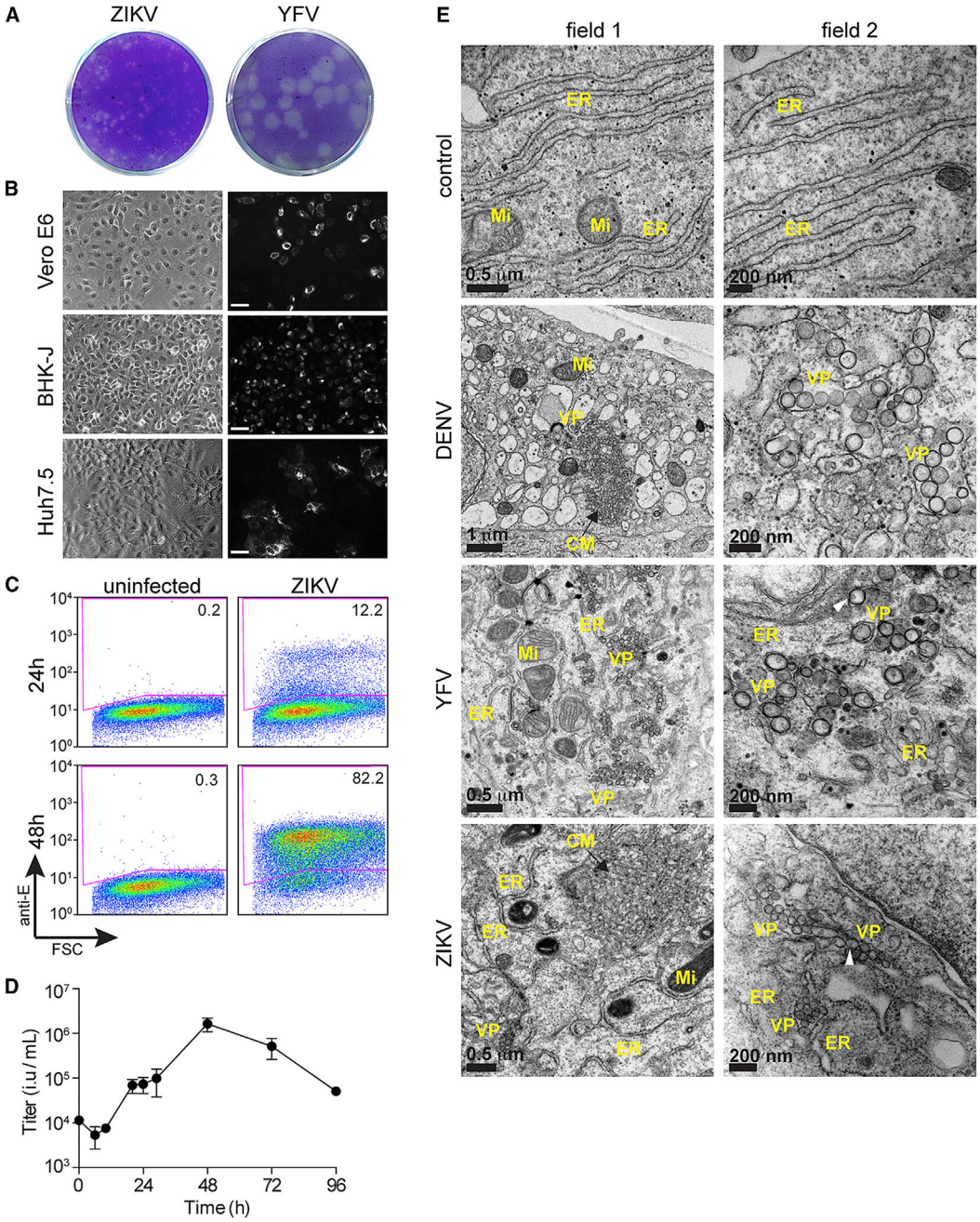

Figure 1. Characterization of a Western ZIKV Isolate in Immortalized Cells

(A) ZIKV and YFV plaque formation on BHK-21J cells 4 days after infection.

(B) Bright-field and indirect immunofluorescence of ZIKV infection (1 MOI) in multiple immortalized cell lines. Cells were stained 48 hr after infection antibody in order to detect ZIKV E protein. Scale bar represents 100 μM.

(C) Quantitation of ZIKV infection in Huh7.5 cells 24 and 48 hr after infection by FACS.

(D) ZIKV growth curve in Huh7.5 cells. Titers at time 0 represent the initial inoculum. Titers at each successive time point represent the accumulation of virus in the supernatant from the previous time point. Results are presented as mean ± SD for duplicate time courses.

(E) Electron micrographs of Huh7.5 cells infected with DENV, YFV, or ZIKV. Two independent fields are show for each condition, with field 2 representing a higher magnification. ER, endoplasmic reticulum; Mi, mitochondria; VP, vesicle packets; and CM, convoluted membranes. White arrows point to membrane invaginations.

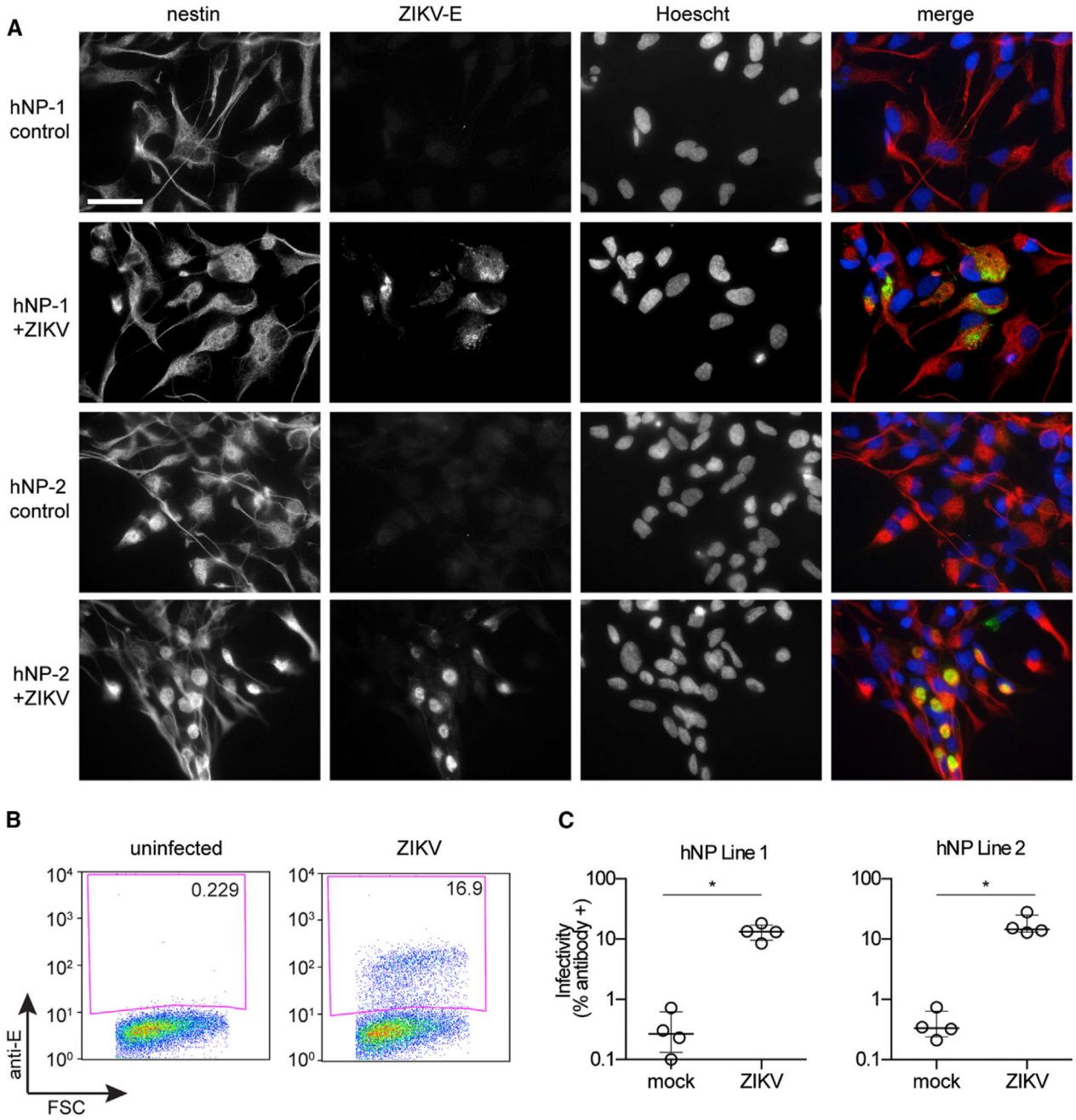

Figure 2. ZIKV Infects Primary Human Fetal Neural Progenitors

(A) Indirect immunofluorescence of ZIKV infection in hNPs. Cells were stained with 4G2 antibody in order to detect ZIKV E protein, anti-nestin antibody to mark neural progenitors, and Hoechst DNA stain. Scale bar represents 50 μM in all panels.

(B and C) Quantitation of ZIKV infection in hNP lines 1 and 2 by FACS. FSC, forward scatter, and Anti-E, antibody staining of ZIKV E. Results are presented as mean ± SD, n = 4.

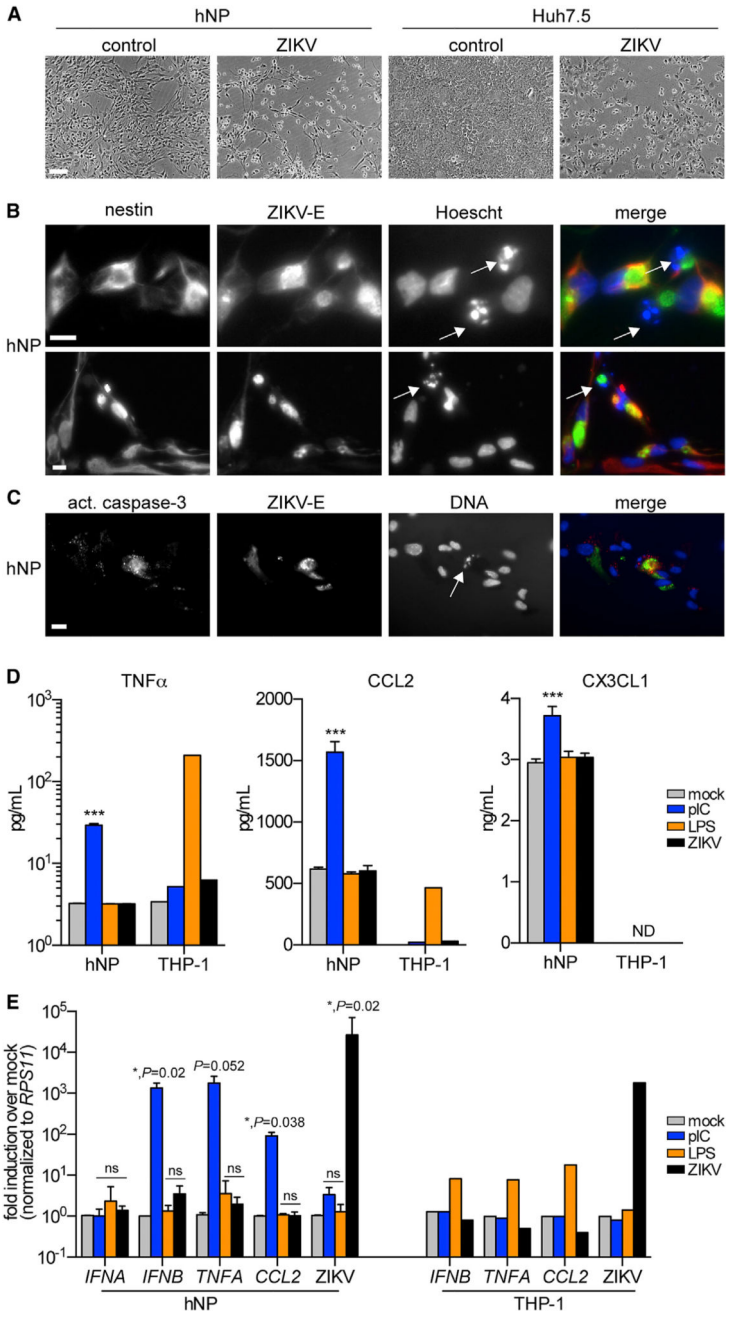

Figure 3. ZIKV Is Partially Cytopathic, but Poorly Immunogenic, in hNPs

(A) Bright-field microscopy images of ZIKV-induced cytopathic effects in hNPs and Huh7.5 cells 4 days after infection. Scale bars represent 200 μM in all panels.

(B) Indirect immunofluorescence of ZIKV infection in hNPs. Cells were stained with antibody in order to detect ZIKV E protein and Hoechst DNA stain. Two representative images from hNP line 1 are shown. Similar results were obtained with hNP line 2.

(C) Indirect immunofluorescence of ZIKV infection in hNPs. Cells were stained antibodies in order to detect ZIKV E protein and activated caspase 3. A representative image from hNP line 1 is shown. Similar results were obtained with hNP line 2. (B and C) White arrows

highlight pyknotic nuclei, and scale bars represent 20 μM in all panels. (D) ELISA to detect TNFα, CCL2, or CX3CL1 in hNP or THP-1 supernatants 24 hr after exposure to pIC (10 μg/ml), LPS (100 ng/ml), or ZIKV (0.5 MOI). ***$p < 0.001$. ND, not detectable.
(E) RT-PCR to detect cytokine mRNA induction or ZIKV RNA in hNP or THP-1 supernatants 24 hr after exposure to pIC, LPS, or ZIKV. Data are normalized to *RPS11* housekeeping control. *$p < 0.05$; ns, not significant.
(D and E) Assays were performed in technical duplicate. Results are presented as mean ± SD, n = 3 for hNP, and n = 1 for THP-1.

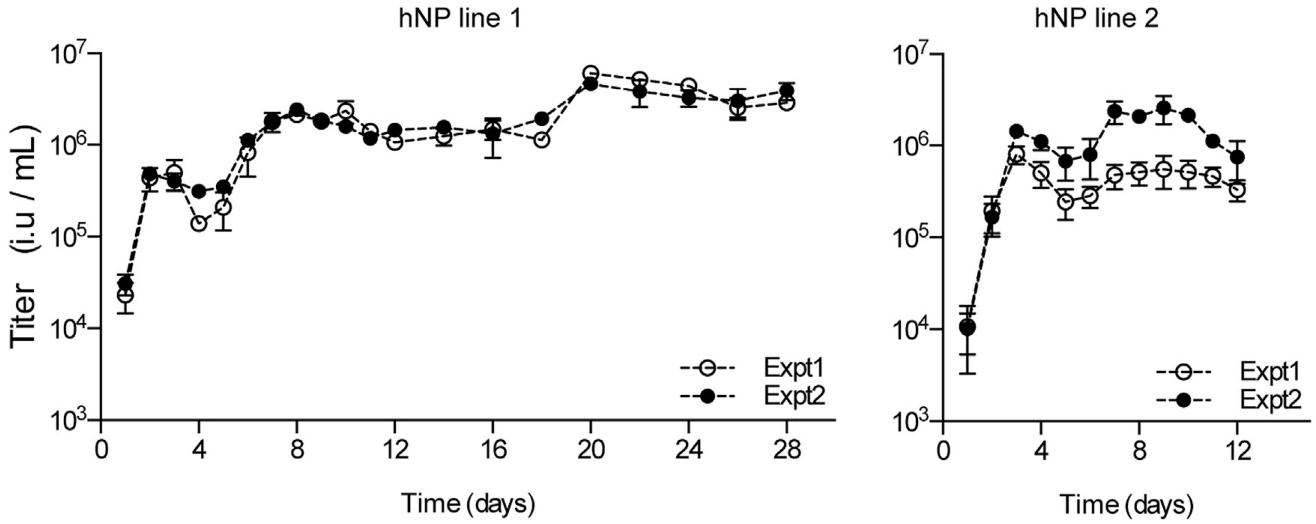

Figure 4. ZIKV Replication Persists Long Term in hNPs

ZIKV growth curves in hNPs. Titers at each time point represent the accumulation of virus in the supernatant from the previous time point. Results from two independent growth curves performed side by side (Expt 1 and Expt 2) in each hNP line are shown. Each supernatant was assayed at three different dilutions in order to determine titers, and data points represent the average of at least two of these titer determinations. Error bars indicate SD.